

Chapter 2

Climate Variability and Change in Tropical South America



Jose Antônio Marengo, Tercio Ambrizzi, Michelle Simões Reboita, Marcos Heil Costa, Claudine Dereczynski, Lincoln Muniz Alves, and Ana Paula Cunha

Abstract This chapter provides definitions of what climate variability and change are and an overview of observed and projected changes in climate in tropical South America. We present a review of the findings of the Intergovernmental Panel on Climate Change (IPCC) from the First Report launched in 1990 until the Sixth Report AR6 released in 2021. This review includes the evolution of models, projections and emission scenarios used by the IPCC since the 1990s. We also include a review of observed long term hydroclimate variability for some key regions in tropical South America that include biomes such as Pantanal, Amazon, the semiarid lands of Northeast Brazil and the Paraná-Plata river basin. For these regions, the focus is on extremes, such as droughts and floods. Temperature, rainfall and drought projections are assessed from the ensemble of global and regional model projections under global warming scenarios of 1.5 and 4.0 °C for various regions of South America. Finally, we also discuss some societal impacts of climate variability and change as well as knowledge gaps that need to be filled with new studies.

Keywords Tropical South America · El Niño · Climate variability · Climate change · Drought · Rainfall

J. A. Marengo (✉) · A. P. Cunha
National Center for Monitoring and Early Warning of Natural Disasters (CEMADEN), São José dos Campos, São Paulo, Brazil
e-mail: jose.marengo@cemaden.gov.br

T. Ambrizzi
University of São Paulo (USP), São Paulo, São Paulo, Brazil

M. S. Reboita
Federal University of Itajubá (UNIFEI), Itajubá, Minas Gerais, Brazil

M. H. Costa
Federal University of Viçosa (UFV), Viçosa, Minas Gerais, Brazil

C. Dereczynski
Federal University of Rio de Janeiro (UFRJ), Rio de Janeiro, Brazil

L. M. Alves
National Institute for Space Research (INPE), São Jose dos Campos, São Paulo, Brazil

2.1 Introduction

2.1.1 *Components of the Climate System*

The climate system corresponds to the interaction among their components: atmosphere, hydrosphere, cryosphere, lithosphere, and biosphere (IPCC 2007, 2013, 2021). Changes in one component directly or indirectly affect the other components and are affected by them. Human-induced climate change already affects several components of the climate system.

The atmosphere is a thin layer that surrounds the Earth and is composed of gases and aerosols that become less dense as the distance from the Earth's surface increases. In this sense, 90% of the atmospheric constituents are within 15 km of Earth's surface, which corresponds to only 1/400 of the radius of Earth (Trenberth 2020). Carbon dioxide (CO₂), ozone (O₃), methane (CH₄) and water vapor (H₂O) are examples of gases with variable concentrations (also referred to as trace gases). Although at small concentrations, these gases are essential for maintaining life, as they contribute to the so-called greenhouse effect. The greenhouse effect is a natural process that has existed since Earth's formation. Without this natural effect, the global mean temperature of the Earth would be $-18\text{ }^{\circ}\text{C}$, which is almost twice as low as its current mean temperature ($\sim 15\text{ }^{\circ}\text{C}$). When solar energy reaches the atmosphere, the atmosphere is not able to absorb a large part of the radiation. The shortwave radiation provided by the Sun is absorbed by the Earth's surface and radiated back as longwave radiation (infrared wavelength). This infrared radiation is absorbed by greenhouse gases such as CO₂ and by clouds (remember that clouds are composed of H₂O). Some of the energy absorbed by the atmospheric constituents will also be radiated back, primarily at infrared wavelengths, in all directions. In this process, the radiation emitted downward from the atmosphere adds to the warming of Earth's surface by solar radiation. This enhanced warming is due to the greenhouse effect. The problem facing the intensification of the greenhouse effect is that anthropogenic actions have contributed to increasing the concentration of the greenhouse gases, therefore increasing the greenhouse effect and the mean temperature of the planet.

The atmosphere interacts with other components of the climate system by means of feedback mechanisms among the climate system components. The feedback mechanisms are also radiative forcings. The term forcing refers to factors that drive or cause changes in the climate system and, as a result, cause climate change. As defined by the IPCC (2013), radiative forcing is a measure of the net change in the energy balance in response to a perturbation. There are three ways to change the radiative balance of the Earth: (a) changing the incoming solar radiation, (b) changing the quantity of solar radiation that is reflected back (albedo) and (c) modifying the amount of longwave radiation that the Earth radiates back to space (changes in the greenhouse gas concentrations) (IPCC 2007). Climate responds to these changes through feedback mechanisms that can either amplify (positive feedback) or decrease (negative feedback) the effects of a change in the climate.

2.1.2 *Natural Climate Variability and Change*

The Earth's climate is determined by the balance between incoming energy from the Sun and outgoing energy emitted by the Earth/atmosphere system. Balance means that what enters in a system leaves this system in the same magnitude. Therefore, changes in the incoming or outgoing energy lead to changes in the climate. However, what are the drivers of these energy changes in addition to the Sun? Before we explain this subject, it is important to define the meaning of climate change and climate variability. According to the glossary of the IPCC (2021):

Climate change: change in the state of the climate that can be identified (e.g., by using statistical tests) by changes in the mean and/or the variability of its properties and that persists for an extended period, typically decades or longer. Climate change may be due to natural internal processes or external forcings, such as modulations of the solar cycles, volcanic eruptions and persistent anthropogenic changes in the composition of the atmosphere or in land use.

Climate variability: change in the state of the climate that can be identified (e.g., by using statistical tests) by changes in the mean and/or the variability of its properties and that persists for an extended period, typically decades or longer. Climate change may be due to natural internal processes or external forcings, such as modulations of the solar cycles, volcanic eruptions and persistent anthropogenic changes in the composition of the atmosphere or in land use.

Changes in climate have occurred even in the absence of humans (IPCC 2021). Therefore, there are natural drivers contributing to these changes that can be internal (components of the climate system) or external (solar luminosity variations, variations in Earth's orbit around the Sun, and volcanic eruptions) to the climate system. The internal drivers change the climate and are affected by the climate (feedback mechanism); on the other hand, the external drivers can only affect the climate and cannot be affected by it (Hartmann 2015). Internal drivers that can lead to climate change are related to modifications in the thermohaline circulation, ice melting and water vapor increase in the atmosphere. However, they are also greatly responsible for climate variability on different time scales (weakly, intraseasonal, seasonal, interannual, and decadal). This variability is associated with teleconnection patterns.

Teleconnection is a term used to refer to local anomalies in the atmosphere, which, in general, are caused by a heat source in the ocean (Trenberth et al. 1998) and that affects the climate of remote places. Thus, teleconnections also refer to local anomalies in the ocean that disturb the climate system (IPCC 2021). We can also think about teleconnection as a perturbation in the climate system caused by its own components. For South America, a description of the main teleconnection patterns that

cause climate variability over South America can be found in Reboita et al. (2021a). In particular, considering an interannual time scale, the most studied and widely known teleconnection pattern is the phenomenon of the El Niño–Southern Oscillation (ENSO). ENSO is an ocean–atmosphere coupled phenomenon that develops in the east and central portions of the tropical Pacific Ocean (Wang et al. 2017; McPhaden et al. 2020). The positive sea surface temperature (SST) anomalies indicate the ENSO warm phase, while the negative anomalies indicate the cold phase (La Niña). During an El Niño event, there is a sea-level gradient with lower values in the eastern Pacific and higher values in the western Pacific, which weakens the trade winds (opposite conditions are observed during a La Niña event). These changes in atmospheric circulation cause anomalous patterns in temperature and precipitation around the globe. Over South America, El Niño episodes are responsible for increased precipitation over southeastern South America and less rainfall over portions of Amazonia and northeast Brazil (Marengo et al. 2017, 2018; McPhaden et al. 2020; Reboita et al. 2021a). The positive SST anomalies during El Niño events can also contribute to boosting global temperatures, increasing global warming in specific years such as 2016 (McPhaden et al. 2020). In climate change scenarios, changes in ENSO are still uncertain, although some models, considering high emission scenarios, indicate that extreme El Niño and La Niña events may double in frequency in the future (Cai et al. 2014, 2015, 2020).

Other important systems may be affected by teleconnection patterns in the Atlantic Ocean sector, such as the North Atlantic Oscillation (NAO), the Southern Annular Mode (SAM) and the Tropical Atlantic SST gradient, which involve variations of opposite signs in the sea-level pressure and SST in both hemispheres (Foltz et al. 2019; Zhang et al. 2021), leading to variations in the position and intensity of the Intertropical Convergence Zone (ITCZ). All these systems and their relationship with teleconnection patterns are well described in Reboita et al. (2021a).

2.1.3 Anthropogenic Climate Change

The Earth’s natural greenhouse effect has been modified by human activities. Humans have increased the concentration of greenhouse gases in the atmosphere, leading to the warming of the Earth’s surface, as a feedback process in the climate system (IPCC 2021). The sources of greenhouse gases can be natural and anthropogenic. H₂O is the most abundant greenhouse gas in the atmosphere. Its concentration increases as the Earth’s atmosphere warms, leading to cloud formation and precipitation. However, the greatest “villain” for increasing the greenhouse effect is CO₂, which has had its concentration greatly increased due to human activities. In 1850, the CO₂ concentration was 280 parts per million (ppm); in August 2021, it reached 416 ppm, thus indicating an increase of approximately 48% during this time interval (<https://climate.nasa.gov/vital-signs/carbon-dioxide/>). When greenhouse gases are injected into the atmosphere, they have long residence times, i.e., the amounts released into the

atmosphere today will remain in the atmosphere for up to two centuries depending on the gas.

Land use changes are also responsible for anthropogenic climate change. When the natural vegetation is changed by agriculture and urbanization, the local albedo is modified as well as the water and energy surface budgets. In the case of urbanization, the large urban centers are also responsible for heat islands that contribute to increasing the air temperature. Agriculture and cattle ranching also contribute to climate change through the release of nitrous oxide (N_2O) available in fertilizers. Another serious issue is deforestation. Forests store large amounts of carbon since trees and other plants absorb carbon dioxide in photosynthesis. Carbon dioxide is converted into carbon and stored in all parts of the plants and the soil. However, the stored carbon is released into the atmosphere in the form of carbon dioxide when the forests are burned or cleared. Rainforests also play an important role in cooling the local climate. As their canopy helps to trap moisture, it leads to slow evaporation, providing a natural air-conditioning effect (Henson 2011). If the forest is removed or burned over large areas, hotter and drier conditions are expected. Studies for South America using climate models, such as Llopart et al. (2018) and Marengo et al. (2021a and references quoted in), have indicated that changing the Amazon Forest to grassland would result in an increase in temperature and in the occurrence of a contrasting spatial pattern on precipitation over Amazonia and changes in the atmospheric circulation for all South America. Increased deforestation may also affect the hydrological cycle in the region, and recent studies by Gatti et al. (2021) have shown that while the Amazon region functions as a sink of CO_2 , the southeastern part of the region, along the so-called deforestation arc, behaves as a source of CO_2 , with temperature increases, rainfall and atmospheric moisture reduction during the last three decades.

Anthropogenic warming has resulted in an expansion of the dry climate areas and a decrease in polar climates. The poleward shift of the Hadley cell could be associated with this impact (Reboita et al. 2019). On the other hand, dry climate regions are more vulnerable to desertification. This causes a loss of biodiversity and reduces agricultural productivity, such as in the semiarid region of Northeast Brazil (Vendruscolo et al. 2021). Marengo et al. (2020 and references quoted in) show that with regional warming above 4 °C, semiarid regions become arid, and the risk of Caatinga vegetation being replaced by arid vegetation is high, which affects the populations in rural areas. On longer time scales, this aridification of the Northeast would lead to land degradation, resulting in a desertification process.

Climate change is also playing an increasing role in determining wildfire regimes (Shukla et al. 2019). In addition to the CO_2 from fires, bacteria in newly exposed soil may release more than twice the usual amount of another greenhouse gas, nitrous oxide, for at least two years. Brazilian biomes (Pantanal, Cerrado, Amazon Forest) suffered much damage from fires in 2019 and 2020 (Henson 2011). A comprehensive review of the increasing fire outbreaks in Brazilian biomes, their contributing causes, overall environmental impacts and consequences for human well-being is provided by Pivello et al. (2021).

2.1.4 Main Concepts in Climate Change and Modeling

Figure 2.1 shows the air temperature frequency distribution for two scenarios: the preindustrial period and present/future time. The difference in mean global temperatures between these two scenarios is represented by a shift to the right of the frequency distribution. At the same time, changes in both tails of the distribution can be seen, which indicates an increase in the frequency of extreme weather events. Thus, in statistical terms, climate extremes can be envisioned as a given probability distribution of a specific event, for example, droughts. Extreme events can be classified as weather extremes or climate extremes. The former refers to systems with short durations, such as intense rain on a specific day; the latter refers to events with longer durations, such as cold waves, heat waves, and droughts.

From observations, we know that our climate is changing, with one example being the frequency, duration and intensity of extreme weather and climate events (IPCC 2021). However, these extremes can also affect the climate itself. Reichstein et al. (2013) highlighted that extremes produce a direct biogeochemical signal in the atmosphere with local concentrations, for instance, of pollution. In other cases, a climate extreme alters the turnover rate of terrestrial carbon pools, leading to prolonged release of CO₂ into the atmosphere, such as the injection of CO₂ into the atmosphere due to vegetation mortality during drought episodes.

To project changes in future climate, numerical climate models are used. Hence, climate models simulate the physical processes taking place in the atmosphere, providing us with data concerning atmospheric circulation, temperature, precipitation, etc. If a model can successfully simulate the main features of atmospheric circulation, the mean state of the climate (average temperature and precipitation) and the frequency of extreme events, it can give us the confidence to apply them to future projections. More details on climate models, scenarios, projections, and uncertainties are shown in Sect. 2.2.

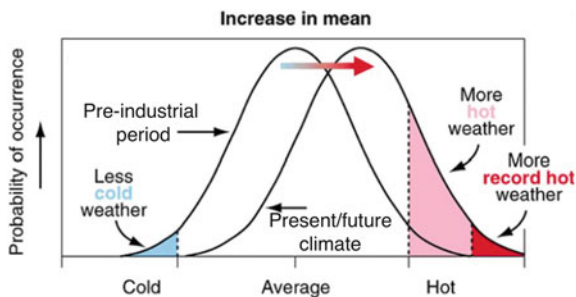


Fig. 2.1 Schematic representation of the probability density function of daily temperature in the preindustrial period and present/future climate

2.2 Climate Modeling: A Primer

2.2.1 *Climate Models: Concepts and Evolution*

Since the 1960s, climate models have evolved a long way until the current state-of-the-art in Earth System Models (ESMs). The first atmospheric models, called atmospheric general circulation models (AGCMs), consisted of physical equations governing atmosphere dynamics, radiative transfer, and other parametrizations. These models were numerically solved using computers and were forced by prescribed boundary conditions such as solar radiation, sea surface temperature, sea ice, and land surface cover. In parallel, oceanic general circulation models (OGCMs) solved similar equations for the ocean and were forced by other boundary conditions, such as air temperature and wind. Climate calculations with a combined Atmosphere–Ocean Model were first performed by Nobelist Syukuro Manabe at the Geophysical Fluids Dynamic Laboratory GFDL (Manabe and Bryan 1969), giving birth to the atmosphere–ocean global climate models AOGCMS.

During the 1990s, global climate models were generally AOGCMs, with horizontal resolutions typically 300–700 km and 12–24 vertical levels in the atmosphere. These models were used in the First and Second Assessment Reports of the IPCC (IPCC 1990, 1995). The use of individual model ensembles (to account for uncertainties in the initial conditions) was rare. In the early 2000s, the first climate system models (CSMs) integrated the four main climate system components. Atmosphere, ocean, land cover, and sea ice were dynamically simulated, varying in time and feedbacking with the other components. In CSMs, the prescribed boundary conditions are solar radiation, aerosols (volcanic and anthropogenic), and atmospheric composition. Typical resolutions at the time were 200 km (horizontal) and 30 levels in the vertical direction for the atmospheric model, and asymmetric resolutions for the oceans, depending on whether it simulates an oceanic current (15–20 km) or not (150–200 km). Land surface and sea ice were usually run at the same resolution as the atmospheric model. These models need to be initialized for at least 30 years until the shallow ocean temperature reaches equilibrium. The use of individual model ensembles became increasingly common (5–100 ensembles). CSMs were the standard in the Third and Fourth IPCC Assessment Reports (IPCC 2001, 2007) and were still used in the Sixth IPCC Assessment Report AR6 (IPCC 2021).

In the late 2000s, the first ESMs were built. In this type of model, the climate system is just a component of the Earth system. In addition to the climate system components, the ESMs explicitly simulate the carbon, water and nitrogen cycles, atmospheric chemistry, and aerosols, directly simulating sea-level rise. CO₂ and aerosol emissions are inputs to the model, and since the full carbon cycle is simulated, the model computes CO₂ concentrations. To do that, these models must be initialized by > 1000 years so that the soil and ocean carbon can reach equilibrium. Not all these characteristics are present in all ESMs, but to be considered an ESM, the model must simulate the full carbon cycle. ESMs are the current standard for the Fifth IPCC AR5 and Sixth IPCC AR6 Assessment Reports (IPCC 2013, 2021), although only a few

models of the Coupled Model Intercomparison Project Versions 5 and 6 (CMIP-5 and -6, respectively) ensembles are fully integrated ESMs. These models have much finer resolutions, sometimes < 100 km for the atmospheric and oceanic models.

Following the evolution of climate models, the attribution of causes of climate change has also been better established:

- The IPCC First Assessment Report (FAR IPCC) (IPCC 1990) concluded that while both theory and models suggested that anthropogenic warming was already well underway, its signal could not yet be detected in observational data against the ‘noise’ of natural variability.
- The IPCC Second Assessment Report (SAR IPCC) stated that the balance of evidence suggests a discernible human influence on global climate. The SAR stated that ‘the balance of evidence suggests a discernible human influence on global climate’ (IPCC 1995).
- The IPCC Third Assessment Report (TAR IPCC) concluded that there is new and stronger evidence that most of the warming observed over the last 50 years is attributable to human activities (IPCC 2001).
- The IPCC Fourth Assessment Report (IPCC AR4) further strengthened previous statements, concluding that most of the observed increase in global average temperatures since the mid-twentieth century is very likely due to the observed increase in anthropogenic greenhouse gas concentrations (IPCC 2007).
- The IPCC Fifth Assessment Report (IPCC AR5) assessed that a human contribution had been detected to changes in warming the atmosphere and ocean; changes in the global water cycle; reductions in snow and ice; global mean sea-level rise; and changes in some climate extremes. AR5 concluded that it is extremely likely that human influence has been the dominant cause of the observed warming since the mid-twentieth century (IPCC 2013).
- The IPCC Sixth Assessment Report (IPCC AR6) establishes that it is unequivocal that human influence has warmed the atmosphere, ocean, and land. Widespread and rapid changes in the atmosphere, ocean, cryosphere and biosphere have occurred (IPCC 2021).

If we are interested in a more precise representation of the local climate, regional climate models (RCMs) are recommended. Their advantage is that they have a higher horizontal resolution (< 50 km) compared to GCMs, being able to better represent aspects of topography, for example. However, RCMs need both initial and spatial boundary conditions, which are provided by GCMs or by reanalysis. A review of the fundamental aspects of GCMs is available in Ambrizzi et al. (2019). With the purpose of establishing a common framework to facilitate the application and comparison of the results obtained with regional climate dynamic and statistical downscaling

and a common protocol for downscaling experiments in different regions of the world, the World Climate Research Program (WCRP) established the Coordinated Regional Climate Downscaling Experiment (CORDEX) in the late 2000s (Giorgi and Gutowski 2015; Giorgi et al. 2021).

2.2.2 Evolution of Climate Emissions Scenarios for IPCC

The IPCC has used a common set of scenarios across the scientific community to provide better comparisons between various studies and to make it easier to communicate model results. In the FAR IPCC (IPCC 1990), idealized emission scenarios were assumed, such as greenhouse gas (GHG) emissions growing at a fixed rate (e.g., 1% a year). Starting with the SAR IPCC (IPCC 1995), a set of six alternative emission scenarios, IS92a-f, were used. These scenarios embodied a wide array of assumptions reflecting how future greenhouse gas emissions might evolve in the absence of climate policies beyond those already adopted (Leggett et al. 1992).

Socioeconomic and emission scenarios are used in climate research to provide plausible descriptions of how variables such as socioeconomic change, technological change, energy, land use, and emissions of greenhouse gases and air pollutants may evolve in the future. They are used as input for climate model runs and as a basis for assessing possible climate impacts, mitigation options, and associated costs. The scenarios from the Special Report on Emission Scenarios (SRES) (Nakicenovic et al. 2000) were used in the TAR IPCC (IPCC 2001) and IPCC AR4 (IPCC 2007) reports. Scenarios were chosen based on our future motivations and emphasis. The A family of scenarios assumes we would focus on economic motivations, while the B family assumes more environmental motivations. Completing the set, family 1 assumed a globalized economy, while family 2 emphasized local communities. The four main scenarios (A1, A2, B1, and B2) considered different futures for global population, global per capita income, per capita energy consumption, and CO₂ emissions per unit of energy produced, with outcomes varying from endless comfort and efficiency (A1) to a return to nature and community (B2), with a sustainable and equitable world in between (B1).

The modeling process using these emissions scenarios follows the sequence: socioeconomic forcings—population, gross domestic product (GDP), and technology—determine GHG and aerosol emissions, which then determine GHG and aerosol concentrations, then radiative forcing, then climate (temperature, precipitation, snow cover, sea ice, sea level, etc.), geophysical impacts (river discharge, fires), and impacts on humans and other species (diseases, heat stress, species distribution, etc.). Although this is a logical way of thinking, the uncertainties in the modeling processes increase from the beginning to the end of the modeling sequence, maximizing uncertainty at the end of the chain.

The IPCC AR5 (IPCC 2013) scenarios modified this modeling sequence, minimizing the uncertainty at the center of the modeling chain, i.e., at the radiative forcing. Scenarios were aggregated at four radiative forcing levels by 2100, above preindustrial levels—2.6, 4.5, 6.0, and 8.5 W/m². Representative concentration pathways (RCPs) were modeled to account for the socioeconomic-technologic emissions and concentration pathways that lead to the selected radiative forcings (van Vuuren et al. 2011).

The IPCC AR6 (IPCC 2021) projected global scenarios based on the shared socioeconomic pathways (SSPs) concept. This new set of scenarios synthesizes knowledge across the physical sciences, impact, adaptation, and mitigation research. The core set of SSP scenarios assumes five main pathways—sustainability (SSP1), regional rivalry (SSP3), inequality (SSP4), development based on fossil fuels (SSP5), and a middle-of-the-road pathway (SSP2). Each pathway is assigned to one or more radiative forcings by 2100 above preindustrial levels: SSP1-1.9, SSP1-2.6, SSP2-4.5, SSP3-7.0, and SSP5-8.5, covering a broad range of emission pathways, including new low-emissions pathways. In IPCC AR6 (IPCC 2021), emissions vary between scenarios depending on socioeconomic assumptions, levels of climate change mitigation, and air pollution controls (for aerosols and nonmethane ozone precursors).

2.2.3 Uncertainties in Model Projections and Model Limitations

The Intergovernmental Panel on Climate Change (IPCC) has used an ensemble of different climate models to address climate system uncertainties and to avoid individual model biases since the TAR IPCC report (IPCC 2001). To standardize comparisons between the different models and their differences in grid type, resolution, and output variables, the climate modeling community developed increasingly sophisticated CMIPs.

Both CMIP3—used in the IPCC AR4 (IPCC 2007)—and CMIP5—used in the AR5 (IPCC 2013) included experiments testing the ability of models to reproduce the twentieth century global surface temperature trends both with and without anthropogenic forcings (GHGs and aerosols). The CMIP6 models used in the IPCC AR6 (IPCC 2021) include new and better representations of physical, chemical, and biological processes and higher model resolution than climate models considered in previous IPCC assessment reports, in addition to improvements in the historical radiative forcings. These enhancements improved the simulation of the last century's mean state of most large-scale indicators of climate change and many other aspects across the climate system (IPCC 2021).

In ESMs, the magnitude of feedback between climate change and the carbon cycle becomes larger but also more uncertain in high CO₂ emissions scenarios (very high

confidence). However, climate model projections show that the uncertainties in atmospheric CO₂ concentrations by 2100 are dominated by the differences between shared socioeconomic pathways, i.e., by humankind's own choices. Additional ecosystem responses to warming do not yet fully included in climate models, such as CO₂ and CH₄ fluxes from wetlands, permafrost thaw, and wildfires which would further increase concentrations of these gases in the atmosphere (IPCC 2021).

In summary, although scenarios are the major source of uncertainty in climate projections, model uncertainty widens the range of possible future climates. These uncertainties include inaccurate representation of interannual and interdecadal modes of climate system variability and misrepresentation of parametrizations and feedbacks, mainly those related to clouds. Another example is the impossibility of modeling the occurrence of random climate-relevant events, such as volcanic eruptions.

2.3 Observed and Projected Climate Scenarios in Tropical South America

2.3.1 *Observed Changes: A Summary*

In the upcoming subsections, a review of climate trends is presented for some regions of Brazil. These regions correspond to Brazilian biomes (Fig. 2.2): the Amazon biome in the Amazon River basin, the Caatinga biome in the semiarid lands of Northeast Brazil, the Pantanal biome, and the Parana-La Plata River basin that covers parts of the Cerrado, Atlantic Forest and Pampas biomes.

To study rainfall variability, we consider the standardized precipitation index (SPI). The SPI is a drought index proposed by McKee et al. (1993) to quantify the probability of occurrence of a precipitation deficit at a specific monthly time scale. To calculate the SPI, precipitation data are fitted to a gamma probability distribution function, and then the inverse normal distribution function is used to rescale the probability values, resulting in SPI values with a mean of zero and a standard deviation of one. As the SPI is a normalized index, it allows the comparison of the index between different locations and climates, which is important for drought monitoring in a large country such as Brazil (Cunha et al. 2019). The time series of SPI-12 months for the regions considered below are shown in Fig. 2.2.

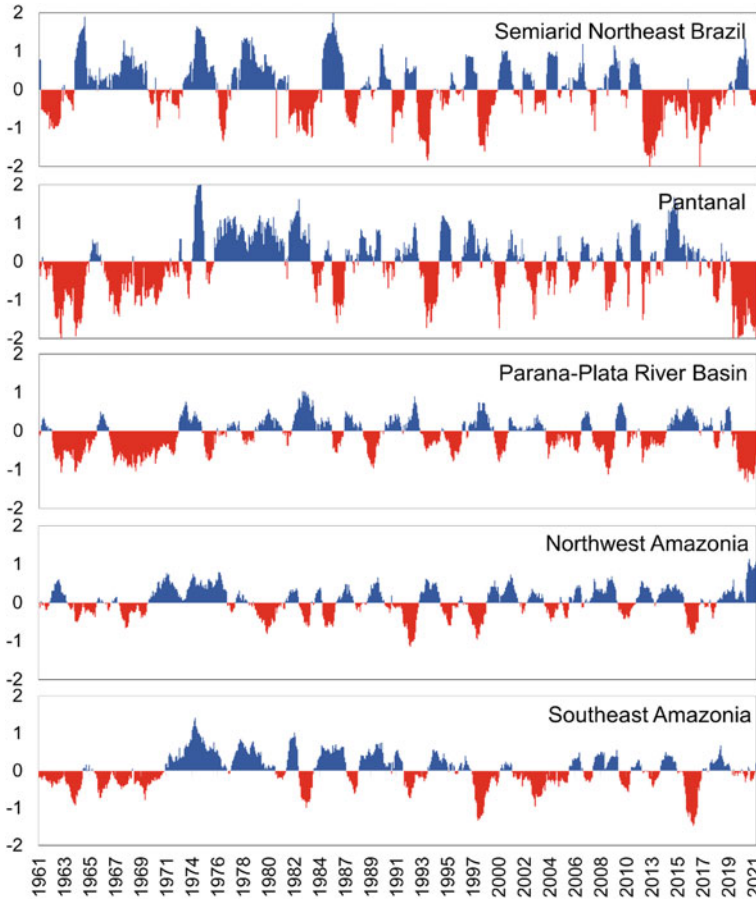


Fig. 2.2 Time series of SPI-12 months for the 5 indicated regions from 1961 to 2021. The regions correspond to the Brazilian biomes. *Source* IBGE-Servico Florestal do Brasil: <https://snif.florestal.gov.br/es/los-biomas-y-sus-bosques/608-florestas-nos-biomas-brasileiros>

2.3.2 *Changes in Rainfall and Hydrology in the Amazon Region*

Historical trends in Amazonian precipitation vary considerably among studies, depending on the dataset, time series period and length, season, and the region evaluated. Most modern rainfall records start in the 1960s, hampering the quantification of trends in the Amazonian region. Studies analyzing rainfall trends in the Amazon for the past four decades show a north–south opposite trend, including increasing rainfall in the northwestern Amazon and a decrease in the southeastern Amazon, particularly in the last decade (Fig. 2.2d and e). These trends may be a consequence of the intensification of the hydrological cycle in the region (Gloor et al. 2013; Barichivich

et al. 2018; Science Panel for the Amazon 2021). The droughts in 1983, 1998, 2010 and 2016 affected the entire Amazon, and the drought in 2005 affected mostly the southern Amazon.

This intensification means increased climate variability, reflected by the increase in recent extreme hydroclimatic events due to stronger northeast trade winds that transport moisture into the Amazon. Recent work by Espinoza et al. (2019) shows that while the southern Amazon exhibits negative trends in total rainfall and extremes, the opposite is found in the northern Amazon, particularly during the wet season. Wang et al. (2018) combined both satellite and in situ observations and revealed changes in tropical Amazonian precipitation over the northern Amazon. Due to increasing rainfall in the northern Amazon, the overall precipitation trend on a basin scale showed a 2.8 mm/year increase for the 1981–2017 period (Paca et al. 2020).

As shown by Schöngart and Junk (2020), water level data for the Rio Negro at Manaus, close to its confluence with the Solimões (Amazonas) River, started being recorded in September 1902. The mean amplitude between the annual maximum (floods) and minimum (droughts) water levels is 10.22 m (1903–2015). Barichivich et al. (2018) indicated a significant increase in the daily mean water level of approximately 1 m over this 113-yr period. Furthermore, the authors observed a fivefold increase in severe flood events resulting in the occurrence of severe flood hazards over the last two decades in the central Amazon (2009, 2012–2015, 2017, 2019 and 2021) and droughts in 2005, 2010, and 2016.

Substantial warming of the tropical Atlantic since the 1990s has played a central role in the region's hydrology, increasing atmospheric water vapor imported by trade winds into the northern Amazon basin and increasing precipitation, especially during the dry-to-wet and wet seasons. The simultaneous cooling of the equatorial Pacific during this period strengthens the Walker circulation and deep convection over the Amazon (Marengo et al. 2021a).

2.3.3 Rainfall and Hydrological Variability in the Pantanal Region

Bergier et al. (2018) used a seasonal rainfall time series from 1926 to 2016 for the Pantanal and found a positive trend in the number of rainy days for all seasons. Lázaro et al. (2020), using a 42-year historical series, found that the number of days without precipitation has greatly increased in the northern Pantanal, as well as the loss of water mass in the landscape over the last 10 years, specifically during the dry season. Overall, currently, the northern Pantanal has 13% more days without rain than in the 1960s (Lázaro et al. 2020). The rainfall during the summers of 2019 and 2020 was well below normal (Fig. 2.2c) and lower than that during the 1970s. For 2020, rainfall was reduced until November. It rained just 160 mm in January, and in March and November, it rained half of the expected value. Since August 2019, rainfall was below normal, and in October 2019, it rained 50 mm (half of the 100 mm average).

This suggests a late onset of the rainy season of the hydrological year 2019–2020 (Marengo et al. 2021b).

Marengo et al. (2021b) showed that the river levels at Ladário represent the hydrological regime of the Upper Paraguay River Basin, which enables the characterization of a given period as drought or flood in the Pantanal. The annual mean level of the Paraguay River at Ladário is 273 cm (1900–2020), ranging from 145 cm in November to 405 cm in June. In terms of the daily absolute maximum, the five events with levels above 600 cm were registered in April 1988 (664 cm) and May 1905 (662 cm). In April 1988, the river level rose to 664 cm, flooding small communities along the river's shores. The year 1970–1971 recorded the largest number of days with levels equal to or below 100 cm during the observation period. On the dry side, the 5 years with the lowest minimum levels were reported in September 1964 (−61 cm), September 1971 (−57 cm), October 1967 (−53 cm), September 1969 (−53 cm), and October 1910 (−48 cm). Negative values indicate observations below the zero level of the river gauge. The lowest values were measured from 1962 to 1973; all 12 years had levels of 100 cm and below. The most recent minimum level value was −32 cm in October 2020. This is the lowest level in 49 years since the previous lowest minimum in 1971. This is consistent with the SPI values from Fig. 2.2c showing negative SPI values in those years.

2.3.4 Rainfall Variability in Northeast Brazil

Northeast Brazil (NEB) is under the influence of Atlantic trade winds that converge along the Intertropical Convergence Zone (ITCZ). The meridional migration of the ITCZ in the semiarid region of NEB determines the rainfall peak season from February to May. Years with drought were observed during El Niño in 1983, 1998 and from 2012–2018 as well as in other years characterized by warm surface waters in the Tropical North Atlantic (Fig. 2.2a). The 2012–2018 drought was associated with a warmer tropical North Atlantic and aggravated by an El Niño event in 2016 (Marengo et al. 2020). Influences from the tropical Pacific Ocean by means of El Niño and from a warmer tropical North Atlantic that moves the ITCZ anomalously to the north are the main causes of rainfall deficiency and drought in the region (Brasil Neto et al. 2021).

The drought that started in 2012 left 1717 municipalities of NEB (96% of total) in a state of emergency, which included rural food insecurity (Marengo et al. 2017, 2020; Brito et al. 2018; Alvala et al. 2019; Cunha et al. 2019; Vieira et al. 2020). During the 2012–2018 drought, the volume of water in the reservoirs on the São Francisco River (Cunha et al. 2019), an important Brazilian river that crosses the region, was reduced to minimal levels. This was coupled with an increase in demand for irrigation water and evaporation from the reservoirs. As a result of the sharp reduction in the São Francisco River flow since 2012, it became necessary to modify the operation of the reservoirs—which were designed in the 1970s—to maintain a

baseflow capable of sustaining the various water uses, mainly the water supply to several cities along the river and large irrigation projects (Marengo et al. 2021a).

2.3.5 Rainfall and Hydrological Variability in the Paraná-La Plata River Basin

Since the 1960s, seven droughts (1977, 1984, 1990, 1992, 2001, 2012 and 2014) have reduced reservoir storage for São Paulo state in Brazil (Fig. 2.2c) (Naumann et al. 2021). In some parts of the La Plata Basin (LPB), such as the Upper Paraná River Basin, severe-to-exceptional hydrological drought conditions have been present since 2014. Nevertheless, in the last two years, 2020–2021, this situation has worsened. Indices of precipitation indicate that the precipitation in the Paraná River basin (Fig. 2.2c) has been below average in recent years (Naumann et al. 2021). Several dry and rainy cycles since the early 1900s have been observed, with the most severe drought on record taking place from December 1968 to September 1971, peaking in March 1969. However, it is important to note that, at that time, the water demand throughout the Paraná River basin was much lower than at present (Cunha et al. 2019). Levels of the Paraná River at Corrientes (Naumann et al. 2021) show that the low levels detected in 2020 and 2021 are comparable to those experienced during the two most severe low-level events in recorded history, i.e., 1934 and 1944.

2.3.6 Cyclones Over the South Atlantic Ocean

Different types of cyclones develop over the South Atlantic Ocean: extratropical, subtropical and tropical (Reboita et al. 2021b, c, e). Extratropical cyclogenesis is the most frequent, and tropical cyclogenesis is the rarest, even though the east coast of Brazil is a region with the potential for tropical cyclogenesis most of the year (Andrelina and Reboita 2021). Extratropical cyclones have a higher frequency in the latitude band of 45° S, whereas subtropical and tropical cyclones occur along the east and south coasts of Brazil. As these systems develop close to the coast, they may cause strong winds, heavy rain and floods.

Projections for the end of the century (2080–2099) under the RCP8.5 scenario through an ensemble with the Regional Climate Model (RegCM4) nested in different CMIP5 global climate models (GCMs) and an ensemble with GCMs indicate (Fig. 2.3): (a) extratropical cyclones over the South Atlantic Ocean are projected to decrease in frequency due to the decrease in near-surface baroclinicity (Reboita et al. 2021c; Marrafon et al. 2022); on the other hand, intensity may be equal to or higher than the historical period (1995–2014), and they can cause more intense rainfall and winds. While the total frequency of extratropical cyclones is projected to decrease, the number of explosive cyclones (deepening rate of ~ 24 hPa/24 h) is

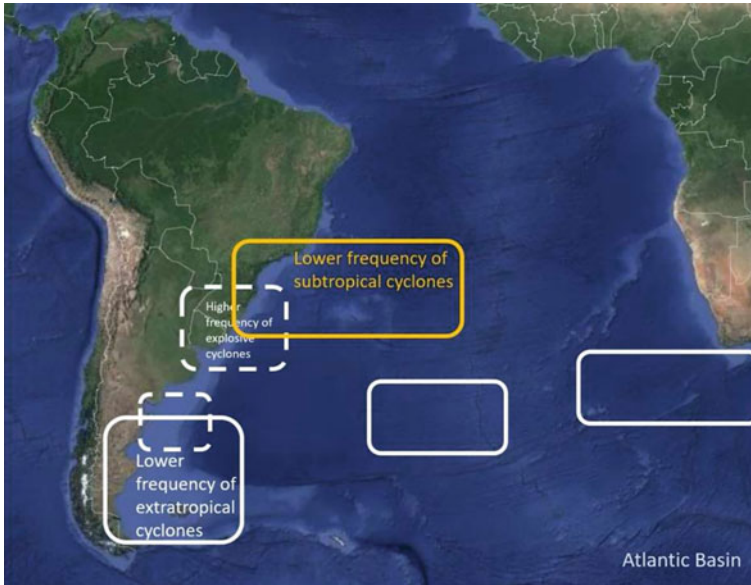


Fig. 2.3 Projected trends in the frequencies of extratropical, explosive and subtropical cyclones at the end of the century (2080–2099) under the RCP8.5 scenario compared to the historical period (1995–2014)

projected to increase (Reboita et al. 2021c); (b) subtropical cyclones are projected to decrease in frequency in part due to the intensification of the South Atlantic subtropical anticyclone (de Jesus et al. 2021; Reboita et al. 2019). On the other hand, intense convection may cause this kind of cyclone to become stronger; and (c) for tropical cyclones, there are no trends in their frequency by the end of the century (Marrafon et al. 2022).

2.3.7 *Changes in Mean Climate and Extremes Based on CMIP6 and CORDEX Models Under Various Levels of Warming (from 1.5 to 4 °C)*

Recent work by Almazroui et al. (2021) shows the results of an analysis of a large ensemble of models from CMIP6 over South America for future changes in slices 2040–2059 and 2080–2099 relative to the reference period (1995–2014) under four shared socioeconomic pathways (SSP1-2.6, SSP2-4.5, SSP3-7.0 and SSP5-8.5). The CMIP6 models successfully capture the main climate characteristics across South America for the reference period. Future precipitation exhibits a decrease east of the northern Andes in tropical South America and the Amazon and an increase over southeastern South America and the northern Andes, consistent with earlier CMIP

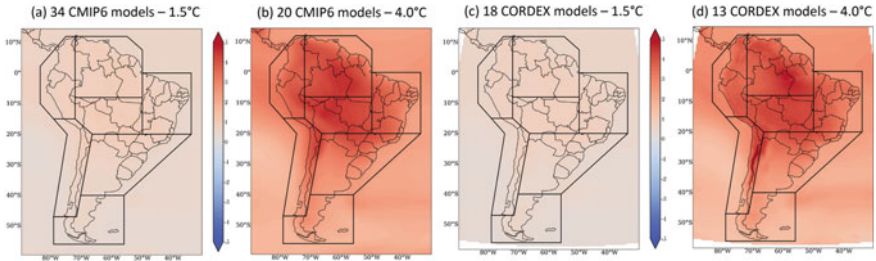


Fig. 2.4 Changes (relative to 1995–2014) in mean annual temperature (T in $^{\circ}\text{C}$) projected by CMIP6 models (under scenario SSP5-8.5) considering 1.5 (a) and 4.0 $^{\circ}\text{C}$ (b) global warming levels and for CORDEX models (under RCP8.5 scenario) and considering 1.5 (c) and 4.0 $^{\circ}\text{C}$ (d) global warming levels (GWLs). Boundaries of IPCC AR6 Atlas regions are shown in the upper left corner of the panel. The same regions are used in Figs. 2.5 and 2.6

(3 and 5) projections. In contrast, temperature increases are robust in terms of magnitude even under SSP1-2.6. Future changes mostly progress monotonically from the weakest to the strongest forcing scenario and from the mid-century to late-century projection period. Furthermore, an increasingly heavy-tailed precipitation distribution and a rightward shifted temperature distribution provide strong indications of a more intense hydrological cycle as greenhouse gas emissions increase. The authors found no clear systematic linkage between model spread about the mean in the reference period and the magnitude of simulated subregional climate change in the future period.

In this subsection, we consider the Northern South America (NSA) and South American Monsoon (SAM) AR6 regions to represent the Amazon Basin and the Northeastern South America (NES) AR6 region to represent Northeast Brazil (Iturbide et al. 2021) (Fig. 2.4). Various levels of warming are considered. For tropical South America, we also include Southeastern South America (SES) so that the entire region (tropical South America) is treated as NSA, SAM, NES and SES. In addition, we are working under a new methodology, employing global warming levels (GWLs) (1.5, 2.0, 3.0, and 4.0 $^{\circ}\text{C}$), instead of decades. Nevertheless, it is important to highlight that such levels of warming can be translated in terms of time (decades), as demonstrated by Seneviratne et al. (2021). For example, the 1.5 $^{\circ}\text{C}$ GWL (relative to the recent past, 1995–2014) will be achieved around the 2050s under the SSP5-8.5 scenario, while the 4.0 $^{\circ}\text{C}$ GWL will be achieved around the 2090s using SSP5-8.5 (see Table 4.2 in Chap. 4—IPCC 2021). Considering the preindustrial period (1850–1900), the 1.5 $^{\circ}\text{C}$ GWL will be reached in 2030 for all scenarios.

2.3.8 Temperature Projections

The mean temperature (T), minimum temperature (TN), and maximum temperature (TX) are used to assess the change in the average temperature magnitude. The

minimum of minimum temperatures (TNn) and the maximum of the maximum temperatures (TXx) are used to evaluate the change in the extreme temperature magnitudes, while days with TX above 35 °C (TX35) and days with TX above 40 °C (TX40) are used to assess the changes in the frequency of warm temperature extremes. The enhanced warming over high-latitude oceans is apparently attributed to the positive snow and sea ice albedo feedback effect in these regions (Goosse et al. 2018). The smallest warmings occur in the tropical region of both hemispheres.

Table 2.1 summarizes projections of changes in air temperature and its extremes for NSA, SAM, NES and SES considering 1.5 and 4.0 °C GWLs under the SSP5-8.5 (RCP8.5) scenario for CMIP6 (CORDEX) models relative to 1995–2014. For the 1.5 °C GWL, the NSA, SAM, NES and SES heat up approximately half of that value (approximately 0.7 °C). However, as the level of warming rises, this difference is reduced. For the 4.0 °C GWL, in the NSA, SAM, NES, and SES, the temperature increases between 2.9 and 4.2 °C in the CMIP6 and CORDEX models. The same behavior is observed for TN, TX, TNn and TXx. Regarding the frequency of warm extremes (TX35 and TX40), the increase from 1.5 to 4.0 GWLs are very high, mainly for SAM, where it will reach almost 92 (107) days with TX above 40 °C, considering CMIP6 (CORDEX) results.

Both the projected magnitude of warming and the frequency of occurrence of hot extremes are higher for SAM than for all South American regions (Fig. 2.4). This feature is also presented in Chou et al. (2014), Reboita et al. (2014), López-Franca et al. (2016), Teichmann et al. (2021) and Coppola et al. (2021). Chou et al. (2014), using the Eta Regional Climate Model forced by two global climate models, HadGEM2-ES and MIROC5, under two RCP scenarios (8.5 and 4.5), show that in the future, the major warming area will be located in the central part of Brazil. In Coppola et al. (2021) and Teichmann et al. (2021), the results from two regional models nested in three GCMs from CMIP5 and RCP2.6 and RCP8.5 show the most warming over the NSA, SAM and NES. López-Franca et al. (2016), using 4 RCMs driven by 3 GCMs and projections for 2079–2098, show greater increases in warm nights and warm days over northern South America. Additionally, Reboita et al. (2014) projections, using RegCM3 nested in ECHAM5 and HadCM3 MCGs under the A1B scenario, indicate general warming throughout all South American regions and seasons, which is more pronounced in the far-future period.

According to the IPCC (2021), it is virtually certain, compared with the recent past (1995–2014) and compared to the preindustrial period (1850–1900), that all of South America will have an increase in the intensity and frequency of hot extremes and a decrease in the intensity and frequency of cold extremes under a 4.0 °C GWL. Additionally, according to this report, it is virtually certain that the mean air temperature will rise across all of South America, with the largest increases occurring in the Amazon Basin (NSA and SAM).

Table 2.1 Changes in the magnitude and frequency of temperature indices for 1.5 and 4.0 °C GWLs using CMIP6 models under the SSP5-8.5 scenario and CORDEX models under the RCP8.5 scenario

Temperature index and unit	AR6 region	1.5 °C		4.0 °C	
		CMIP6	CORDEX	CMIP6	CORDEX
<i>T</i> (°C)	NSA	0.8 (0.2–1.2)	0.7 (0.5–1.1)	3.8 (3.1–4.5)	3.2 (3.2–4.8)
	NES	0.7 (0.3–1.1)	0.7 (0.4–1.0)	3.1 (2.7–3.6)	3.5 (3.0–4.3)
	SAM	0.8 (0.3–1.3)	0.8 (0.5–1.2)	3.9 (3.2–4.6)	4.2 (3.4–5.0)
	SES	0.6 (0.2–0.9)	0.6 (0.3–0.8)	3.0 (2.5–3.4)	2.9 (2.4–3.5)
TN (°C)	NSA	0.7 (0.2–1.1)	0.7 (0.4–1.1)	3.6 (3.0–4.3)	3.4 (2.9–4.0)
	NES	0.6 (0.2–1.0)	0.7 (0.4–1.0)	3.1 (2.5–3.8)	3.2 (2.6–3.7)
	SAM	0.8 (0.3–1.3)	0.8 (0.5–1.1)	4.0 (3.4–4.6)	4.0 (3.2–4.7)
	SES	0.6 (0.2–0.9)	0.6 (0.3–0.8)	3.1 (2.4–3.5)	3.0 (2.5–3.6)
TX (°C)	NSA	0.9 (0.2–1.4)	0.8 (0.5–1.1)	4.2 (3.3–5.2)	3.9 (3.0–5.0)
	NES	0.8 (0.2–1.3)	0.7 (0.4–1.0)	3.8 (3.1–4.6)	3.3 (2.9–3.8)
	SAM	0.9 (0.3–1.6)	0.9 (0.5–1.3)	4.5 (3.4–5.5)	4.4 (3.5–5.2)
	SES	0.7 (0.1–1.1)	0.6 (0.2–0.9)	3.1 (2.2–3.8)	2.9 (2.3–3.5)
TNn (°C)	NSA	0.7 (0.2–1.0)	0.7 (0.4–1.1)	3.5 (2.6–4.4)	3.8 (3.1–4.5)
	NES	0.7 (0.3–0.9)	0.6 (0.4–0.9)	3.2 (2.6–4.1)	3.3 (2.6–3.7)
	SAM	0.8 (0.3–1.3)	0.7 (0.3–1.1)	3.7 (2.9–4.5)	4.1 (3.1–5.1)
	SES	0.6 (0.2–1.2)	0.5 (0.0–0.8)	2.9 (2.4–3.4)	2.6 (1.7–3.2)
TXx (°C)	NSA	1.0 (0.3–1.6)	0.9 (0.5–1.2)	4.5 (3.7–5.2)	4.2 (3.3–5.0)
	NES	0.9 (0.3–1.6)	0.8 (0.5–1.2)	3.9 (3.3–4.5)	3.9 (3.4–4.3)
	SAM	1.3 (0.4–2.4)	1.2 (0.6–1.9)	6.1 (4.3–8.0)	5.5 (4.3–7.0)
	SES	0.9 (0.4–1.4)	0.8 (0.3–1.3)	4.1 (3.2–5.0)	3.9 (3.1–4.5)
TX35 (days)	NSA	16.1 (1.7–28.4)	18.1 (7.1–26.6)	89.7 (33.0–109.1)	98.1 (69.3–122.1)
	NES	8.5 (1.7–24.8)	10.5 (3.8–25.6)	43.3 (33.9–100.3)	57.5 (33.9–87.3)
	SAM	17.8 (4.5–31.4)	20.1 (9.6–37.3)	91.7 (43.3–153.0)	106.7 (80.7–132.4)
	SES	5.7 (1.9–10.7)	6.0 (1.0–9.1)	28.2 (16.6–36.2)	34.1 (19.8–47.5)
TX40 (days)	NSA	4.3 (0.0–16.1)	6.0 (0.0–12.9)	39.2 (1.6–77.7)	52.6 (11.0–104.9)
	NES	1.9 (0.0–9.7)	1.8 (0.1–4.6)	18.4 (0.8–37.1)	21.6 (5.7–43.3)

(continued)

Table 2.1 (continued)

Temperature index and unit	AR6 region	1.5 °C		4.0 °C	
		CMIP6	CORDEX	CMIP6	CORDEX
	SAM	3.9 (0.2–13.1)	8.5 (1.5–17.8)	29.4 (4.1–55.2)	57.0 (28.5–101.2)
	SES	2.3 (0.4–5.2)	1.4 (0.2–2.3)	10.8 (6.0–19.4)	12.6 (5.4–22.1)

Source Interactive Atlas—IPCC AR6 (Iturbide et al. 2021)

Displayed are median values and, in parentheses, the 5–95% ranges over NSA, SAM, NES, and SES relative to the period 1995–2014

2.3.9 Precipitation Projections

The total precipitation (PR) is used to indicate the change in the amount of precipitation, and the maximum 1-day and 5-day precipitation (RX1day and RX5day) are used to show the change in the magnitude of precipitation extremes. Unlike the results for temperature, precipitation and its extremes exhibit a more heterogeneous behavior and, in most regions, with no agreement between the models (see precipitation global maps at <https://interactive-atlas.ipcc.ch/>). Moreover, for the near future (2021–2040) or for the low GWLs (1.5 °C and 2.0 °C), even considering the most pessimistic scenarios (SSP5-8.5 and RCP8.5), the sign of change is very weak, with no agreement between models. Figure 2.5 presents the change in annual precipitation (PR) for 1.5 and 4.0 °C GWLs relative to 1995–2014 using CMIP6 and CORDEX models under the SSP5-8.5 and RCP8.5 scenarios, respectively. The only robust signs of projected changes in annual precipitation and where there is an agreement between the models (Fig. 2.5b and d) occur in the east of the NSA, with a 12% reduction (median) in PR, as well as in southwestern South America (SWS). Projections of increases in PR are observed over SES and in the extreme west of northwestern South America (NWS). The drying (wetting) conditions over NSA and SAM (SES) are also presented in Chou et al. (2014), Llopart et al. (2014), Reboita et al. (2014), Coppola et al. (2021), Teichmann et al. (2021), and Teodoro et al. (2021).

Chou et al. (2014) showed a reduction in summer precipitation over northern and central South America and an increase in PR over southern South America. Llopart et al. (2014), using the regional climate model RegCM4 driven by the HadGEM, GFDL and MPI GCMs under RCP8.5 and, more recently, Teodoro et al. (2021), have also shown projections of reduced precipitation over the broad Amazon and central Brazil region and increased precipitation over the La Plata basin and central Argentina. According to Llopart et al. (2014), the tendency toward an extension of the dry season over central South America is due to a late onset and an early retreat of the SAM. Reboita et al. (2014) also projected dry conditions in all seasons over northern South America and an increase in precipitation over the SES mainly in spring and summer. More recent work by Coppola et al. (2021) points out that extreme wet and flood prone maxima are projected to increase over the La Plata basin (SES).

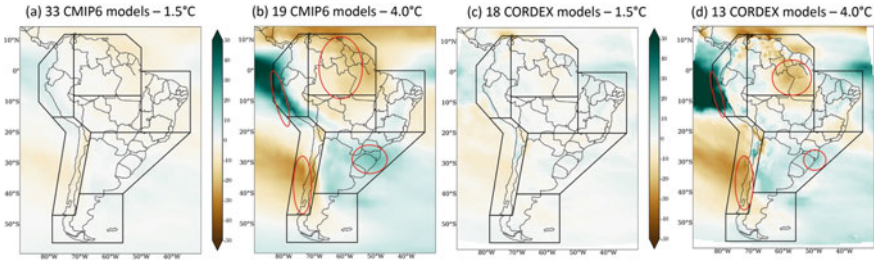


Fig. 2.5 Changes (relative to 1995–2014) in mean annual precipitation (PR, in %) projected by CMIP6 models (under scenario SSP5-8.5) considering 1.5 (a) and 4.0 °C (b) GWLs and for CORDEX models (under RCP8.5 scenario) considering 1.5 (c) and 4.0 °C (d) GWLs. GWLs. Red circles and ellipses indicate areas with robust signs of projected changes in annual precipitation and where there is an agreement between the models. See Fig. 2.4 for names of regions delimited in figure

Regarding the behavior of the magnitude of extreme precipitation (RX1day and RX5day), there is an increase over most of South America, including the Amazon and Northeast Brazil. It is important to highlight that extreme precipitation is determined by local exchanges in heat, moisture, and other related quantities (thermodynamic changes) and those associated with atmospheric and oceanic motions (dynamic changes) (Seneviratne et al. 2021). The increase in water vapor leads to robust increases in precipitation extremes everywhere, with a magnitude that varies between 4 and 8% per degree Celsius of surface warming (thermodynamic contribution) (Fischer and Knutti 2016; Sun et al. 2020). However, the dynamic contributions show large differences across models and are more uncertain than thermodynamic contributions (Shepherd 2014; Trenberth et al. 2015; Pfahl et al. 2017).

Increases in extreme precipitation magnitude and frequency over NSA, SAM, NES, and SES are projected for the end of the century using a 4 °C GWL (Li et al. 2021). However, using RCMs, Chou et al. (2014) and Coppola et al. (2021) projected negative changes in precipitation extremes over the NSA. Regarding SAM, NES, and SES, Coppola et al. (2021) project positive changes, while Chou et al. (2014) project negative changes, except for SES.

In summary, IPCC (2021) projections indicate that for mean precipitation there will be a drying (wetting) signal for NSA and NES (SES). IPCC (2021) states that an intensification of heavy precipitation is projected with medium confidence, compared to the recent past (1995–2014) and with the preindustrial period (1850–1900) for 2 and 4 °C GWLs, for NSA, SAM, and NES and particularly for SES.

2.3.10 Drought Projections

Consecutive dry days (CDD) are used to assess changes in meteorological drought. Figure 2.6 presents changes in CDD for 1.5 and 4.0 °C GWLs relative to 1995–2014

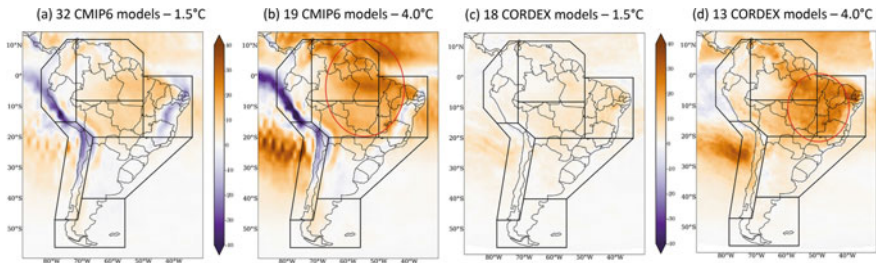


Fig. 2.6 Changes (relative to 1995–2014) in consecutive dry days (CDD, in number of days) projected by CMIP6 models (under scenario SSP5-8.5) considering 1.5 (a) and 4.0 °C (b) GWLs and for CORDEX models (under RCP8.5 scenario) considering 1.5 (c) and 4.0 °C (d) GWLs. See Fig. 2.4 for the names of the regions delimited in the figure

using CMIP6 and CORDEX models under the SSP5-8.5 and RCP8.5 scenarios, respectively. The increase in CDD over the Amazon basin is remarkable, indicating a drier climate in the future, both in CMIP6 and CORDEX models. Over NES, the models also show an increase in CDD. Over the SES, there is no agreement between the models, but the model results show an overall decrease in precipitation at 1.5 °C GWLs. According to Chou et al. (2014), Coppola et al. (2021), and Reboita et al. (2021d), positive changes in CDD over NSA, SAM and NES are projected in the far-future.

2.4 Impacts on Natural and Human Systems

2.4.1 Impacts on Natural Ecosystems

The drought that started in 2012 highlights the vulnerability of NEB. Arid conditions have been detected during recent years mainly in the central semiarid region, covering almost 2% of NEB (Marengo et al. 2020). The projections of vegetative stress conditions derived from the empirical model for the vegetation health index (VHI) are consistent with projections from vegetation models, where semidesert types typical of arid conditions would replace the current semiarid bushland vegetation (“caatinga”) by 2100 (Marengo et al. 2020). Therefore, there is a possibility that under permanent drought conditions with warming above 4 °C, arid conditions would prevail in NEB since 2060, which would lead to land degradation and desertification.

The drought situation in 2019–20 in the Pantanal and the Upper Paraguay River basin has been unusually harsh, with dry and warm conditions favoring the propagation of fires. The increased number of fires affects human activities and biodiversity. These fires and droughts aggravated the situation of vulnerable fauna and flora. Changes in the quality of the rainy season can also affect wetland hydrology,

and droughts can seriously affect the living conditions of biological populations (Marengo et al. 2021a).

Drought and flood events in Amazonia have produced impacts such as an increased risk of forest fires, extreme warming, floods and inundations, which can affect the human population and flora and fauna both on land and in lakes and rivers (Davidson et al. 2012; Marengo et al. 2013; Brando et al. 2014; Doughty et al. 2015). While droughts increase the risk of tree mortality, the combination of severe droughts and floods can put additional stress on Amazon forests, especially if the flooding regime of regularly inundated areas is perturbed outside of their natural range (Langerwisch et al. 2013). It also affects riverine carbon balance by outgassing carbon from the Amazon River and the amount exported to the Atlantic Ocean, with nonlinear effects to be expected if deforestation is also considered (Langerwisch et al. 2016).

2.4.2 Potential Impacts on Society

Due to the impacts of the 2012–2017 drought in NEB, public policies have been implemented to reduce social and economic vulnerability for small farmers. In the long term, to make the semiarid region less vulnerable to drought, strengthened integrated water resource management and a proactive drought policy are needed to restructure the economy. Integrating drought monitoring and seasonal climate forecasting provides a means of assessing the impacts of climate variability and change, leading to disaster risk reduction through early warning. In a future scenario with a high risk of drought and possible desertification in regions with warming above 4 °C, agricultural activities can be affected by severe water stress and may be devastating for local populations. This condition can make drought irreversible, and prolonged water stress could lead to aridity and land degradation (Marengo et al. 2020).

Changes in the rainfall regime and the flood pulse in the Pantanal are likely to disrupt the processes that maintain these landscapes; furthermore, landscape modification may dramatically alter wetlands (Ivory et al. 2019; Marengo et al. 2021b). Many human activities in the region rely on the ecosystem services provided by the Pantanal, including professional and touristic fishing and contemplative tourism (Bergier et al. 2018). The available land for cattle ranching and farming is dependent on the extent of flooding during each wet season. Due to these flooding events, local ranchers struggle to survive. Because of drought, fires spread and affect the natural biodiversity in the Pantanal region as well as the agribusiness and cattle ranching sectors. The uncontrolled fires occurring in the dry season are of anthropogenic origin. They are directly related to deforestation, cleaning, and reforming pastures. Improper practices and the use of fire as a management practice without control techniques endanger conservation (Aragão et al. 2018; Alho et al. 2019).

It is important to mention that in the Amazon region, the perception of drought and flood by the population may be different when compared to other regions, and low or high river levels are better indicators of drought or floods, respectively, compared

to rainfall anomalies. Through their close dependency on water levels, local people are well placed to detect variability in both climate and hydrological regimes and can respond to early warning signals to cope with potential impacts on their activities (Pinho et al. 2015; Marengo et al. 2018). Development in the Amazon region has pushed the agricultural frontier, resulting in widespread land cover change. As agriculture in the region has low productivity and is unsustainable, the loss of biodiversity and continued deforestation will lead to high risks of irreversible changes in Amazon forests (Nobre et al. 2016).

2.4.3 Governance Actions to Mitigate Climate Change: Examples for Northeast Brazil (NEB) and Amazon

In this section, we focus on two regions of South America that have high social and biodiversity vulnerability in tropical South America, NEB and Amazon, respectively. In NEB, current-drought emergency relief measures include water distribution by trucks (“carros pipa”), plus cash transfer and state-sponsored microinsurance programs for smallholders (Magalhães 2016). Actions are heavily concentrated on water distribution, initially to rural but also to urban and coastal communities that depend upon water supply originating in the semiarid regions. In addition, recent anti-poverty programs, such as education, health and extreme poverty alleviation, have significantly improved the life conditions in the region (Alvala et al. 2019; Marengo et al. 2020). Despite significant improvement in quality-of-life indicators in the past 15 years, levels of vulnerability remain high, especially in rural households that are more dependent on agriculture (Engle and Lemos 2010). In a recent work, Marengo et al. (2021c) presented a list of initiatives that can be considered adaptation options to cope with drought in NEB in the long term. Some are technical options, while others can be considered more political. However, others are related to monitoring and early warning of drought and seasonal climate forecasts from national and regional agencies. The target of all these actions is the protection of vulnerable populations and small-scale farming in the semiarid region of NEB.

The challenges of governance of climate change in the Amazon region are related to the fact that even though the region will be impacted, drivers of deforestation are linked to economic activities such as logging, cattle ranching, soy harvesting, and mining, as well as to public investments in infrastructure such as roads and hydropower plants (Science Panel for the Amazon 2021), all of which have played a significant role in the economic growth of the region and of Brazil.

Amazonian municipalities of Brazil are involved in global climate governance. The actions are linked to the national policy to control deforestation. Other actions can be characterized by the initiatives taken by municipalities to become involved in international negotiation processes focusing on the United Nations Framework Convention on Climate Change (UNFCCC) and the Reducing Emissions from Deforestation and Forest Degradation (REDD+) mechanisms. These initiatives have strengthened

subnational, national, regional and transnational networks and have created commitments to mitigate and find ways to adapt to global climate change. This is relevant to the goals of deforestation reduction proposed by Brazil during the Paris Agreement in 2015 (IPCC 2021).

2.5 Gaps, Limitations and Future Lines of Work

With the likelihood of more frequent droughts, there is a need for a better perception that adaptive capacity is still low, as shown by the consequences of recent droughts in tropical South America. Science has assembled enough knowledge to underline the global and regional importance of the Amazon, Pantanal and Parana-Prata regions, which can support policy-making to keep these sensitive ecosystems functioning. This major challenge requires substantial resources and strategic cross-national planning and a unique blend of expertise and capacities established in the regions' countries and from international collaboration. While science can still advance further in this area, we have also assembled enough knowledge to underline the global and regional importance of an intact Amazon region to support policy-making and to keep this sensitive ecosystem functioning. Measures and strategies for drought preparedness could be strengthened by regional, national and international financing mechanisms to provide for disaster risk reduction and disaster risk management in the long term.

A multiannual drought has been affecting the Plata Basin since mid-2019. The lack of rainfall, mainly in the upper part of the basin, has led to a considerable decrease in the flow of the Paraguay and Paraná rivers. Due to its prolonged duration and severity, this drought has already produced many impacts on several different socioeconomic sectors and has also severely affected ecosystems. These include water supply disruptions, forest fires, reduced agricultural yields, decreased river transport on the Paraguay and Paraná rivers, and a considerable reduction in hydroelectric energy production (Naumann et al. 2021). The impacts of this drought need to be assessed in the context of cross bordering collaboration.

On the governance side, governments and institutions are critical determinants of adaptive capacity and resilience in NEB, from the municipal to the federal levels. Other actions on the scientific side include preventive activities, such as risk monitoring and early warning systems for weather and climate extremes that can trigger natural disasters that would impact human and natural systems. These actions include seasonal climate forecasts for the region, spanning from model development to risk communication to the public and decision-makers. Also, it is necessary to consolidate disaster risk management in Brazil, which requires exploring synergies between all the institutions involved. It is necessary to create mechanisms for the integration and articulation of technical and scientific knowledge of the various dimensions of risk by ensuring a linkage between policies related to disaster risk reduction, climate change adaptation, and the UN Sustainable Development Goal 13 (Climate Action).

Acknowledgements This research was funded by the National Institute of Science and Technology for Climate Change Phase 2 under CNPq, grant number 465501/2014-1; Fundação de Amparo à Pesquisa do Estado de São Paulo (FAPESP) grant numbers 2014/50848-9 and 2017/09659-6; the National Coordination for High Level Education and Training (CAPES), grant number 88887.136402/2017-00; and CNPq grant 301397/2019-8 for José A. Marengo and Tercio Ambrizzi. It was partially funded by the Project Rede Pantanal from the Ministry of Science, Technology and Innovations of Brazil (FINEP grant 01.20.0201.00). Tercio Ambrizzi also had partial support from CNPq 301397/2019-8. Michelle Reboita was funded by CNPq grants 306488/2020-5 and 420262/2018-0.

References

- Alho CJR, Mamede SB, Benites M et al (2019) Threats to the biodiversity of the Brazilian Pantanal due to land use and occupation. *Ambiente & Sociedade*. <https://doi.org/10.1590/1809-4422asoc201701891vu2019L3AO>
- Almazroui M, Ashfaq M, Islam MN et al (2021) Assessment of CMIP6 performance and projected temperature and precipitation changes over South America. *Earth Syst Environ* 5:155–183. <https://doi.org/10.1007/s41748-021-00233-6>
- Alvala R, Cunha AP, Brito SS et al (2019) Drought monitoring in the Brazilian Semiarid region. *An Acad Bras Ciênc*. <https://doi.org/10.1590/0001-3765201720170209>
- Ambrizzi T, Reboita MS, da Rocha RP et al (2019) The state of the art and fundamental aspects of regional climate modeling in South America. *Ann N Y Acad Sci* 1436:96–120. <https://doi.org/10.1111/nyas.13932>
- Andrelina B, Reboita MS (2021) Climatologia do Índice do Potencial de Gênese de Ciclones Tropicais nos Oceanos Adjacentes à América do Sul. *An Inst Geociências*. https://doi.org/10.11137/1982-3908_2021_44_39515
- Aragão LEOC, Anderson LO, Fonseca MG et al (2018) 21st century drought-related fires counteract the decline of Amazon deforestation carbon emissions. *Nat Commun*. <https://doi.org/10.1038/s41467-017-02771-y>
- Barichivich J, Gloor E, Peylin P et al (2018) Recent intensification of Amazon flooding extremes driven by strengthened Walker circulation. *Sci Adv*. <https://doi.org/10.1126/sciadv.aat8785>
- Bergier I, Assine ML, McGlue MM et al (2018) Amazon rainforest modulation of water security in the Pantanal wetland. *Sci Total* 619–620:1116–1125. <https://doi.org/10.1016/j.scitotenv.2017.11.163>
- Brando PM, Balch JK, Nepstad DC et al (2014) Abrupt increases in Amazonian tree mortality due to drought-fire interactions. *PNAS* 111(17):6347–6352. <https://doi.org/10.1073/pnas.1305499111>
- Brasil Neto RM, Santos CAG, Silva JFCB et al (2021) Evaluation of the TRMM product for monitoring drought over Paraíba State, northeastern Brazil: a trend analysis. *Sci Rep*. <https://doi.org/10.1038/s41598-020-80026-5>
- Brito SSB, Cunha APMA, Cunningham CC et al (2018) Frequency, duration and severity of drought in the Semiarid Northeast Brazil region. *Int J Climatol* 38(2):517–529. <https://doi.org/10.1002/joc.5225>
- Cai W, Borlace S, Lengaigne M et al (2014) Increasing frequency of extreme El Niño events due to greenhouse warming. *Nat Clim Change* 4:111–116. <https://doi.org/10.1038/nclimate2100>
- Cai W, Wang G, Santoso A et al (2015) Increased frequency of extreme La Niña events under greenhouse warming. *Nat Clim Change* 5:132–137. <https://doi.org/10.1038/nclimate2492>
- Cai W, McPhaden M, Grimm AM et al (2020) Climate impacts of the El Niño-Southern Oscillation on South America. *Nat Rev Earth Environ* 1:215–231. <https://doi.org/10.1038/s43017-020-0040-3>

- Chou SC, Lyra A, Mourão C et al (2014) Evaluation of the Eta simulations nested in three global climate models. *Am J Clim Change* 3:438–454. <https://doi.org/10.4236/ajcc.2014.35039>
- Coppola E, Raffaele F, Giorgi F et al (2021) Climate hazard indices projections based on CORDEX-CORE, CMIP5 and CMIP6 ensemble. *Clim Dyn* 57:1293–1383. <https://doi.org/10.1007/s00382-021-05640-z>
- Cunha APMA, Zeri M, Deusdará Leal K et al (2019) Extreme drought events over Brazil from 2011 to 2019. *Atmosphere*. <https://doi.org/10.3390/atmos10110642>
- Davidson EA, de Araújo AC, Artaxo P et al (2012) The Amazon basin in transition. *Nature* 481:321–328. <https://doi.org/10.1038/nature10717>
- Doughty CE, Metcalfe DB, Girardin CAJ et al (2015) Drought impact on forest carbon dynamics and fluxes in Amazonia. *Nature* 519:78–82. <https://doi.org/10.1038/nature14213>
- Engle NL, Lemos MC (2010) Unpacking governance: building adaptive capacity to climate change of river basins in Brazil. *Global Environ Change* 20:4–13. <https://doi.org/10.1016/j.gloenvcha.2009.07.001>
- Espinoza JC, Ronchail J, Marengo JA et al (2019) Contrasting North-South changes in Amazon wet-day and dry day frequency and related atmospheric features (1981–2017). *Clim Dyn* 52:5413–5430. <https://doi.org/10.1007/s00382-018-4462-2>
- Fischer EM, Knutti R (2016) Observed heavy precipitation increase confirms theory and early models. *Nat Clim Change* 6:986–991. <https://doi.org/10.1038/nclimate3110>
- Foltz GR, Brandt P, Richter I et al (2019) The tropical Atlantic observing system. *Front Mar Sci*. <https://doi.org/10.3389/fmars.2019.00206>
- Gatti LV, Basso LS, Miller JB et al (2021) Amazonia as a carbon source linked to deforestation and climate change. *Nature* 595:388–393. <https://doi.org/10.1038/s41586-021-03629-6>
- Giorgi F, Gutowski WJ (2015) Regional dynamical downscaling and the CORDEX initiative. *Annu Rev Environ Resour* 40:467–490. <https://doi.org/10.1146/annurev-environ-102014-021217>
- Giorgi F, Coppola E, Jacob D et al (2021) The CORDEX-CORE EXP-I initiative: description and highlight results from the initial analysis. *Bull Am Meteorol Soc*. <https://doi.org/10.1175/BAMS-D-21-0119.1>
- Gloor M, Brienen RJW, Galbraith D et al (2013) Intensification of the Amazon hydrological cycle over the last two decades. *Geophys Res Lett* 40:1729–1733. <https://doi.org/10.1002/grl.50377>
- Goosse H, Kay JE, Armour KC et al (2018) Quantifying climate feedbacks in polar regions. *Nat Commun*. <https://doi.org/10.1038/s41467-018-04173-0>
- Hartmann L (2015) *Global physical climatology*, 2nd edn. Elsevier, Amsterdam
- Henson R (2011) *The rough guide to climate change*. Dorling Kindersley, UK
- IPCC (1990) *Climate change 1990: first assessment report*. Cambridge University Press, Cambridge
- IPCC (1995) *Climate change 1995: the science of climate change. Contribution of Working Group I to the Second Assessment Report of the Intergovernmental Panel on Climate Change*. Cambridge University Press, Cambridge
- IPCC (2001) *Climate change 2001: the scientific basis. Contribution of Working Group I to the Third Assessment Report of the Intergovernmental Panel on Climate Change*. Cambridge University Press, Cambridge
- IPCC (2007) *Climate change 2007: the physical science basis. Contribution of Working Group I to the Fourth Assessment Report of the Intergovernmental Panel on Climate Change*. Cambridge University Press, Cambridge
- IPCC (2013) *Climate change 2013: the physical science basis. Contribution of Working Group I to the Fifth Assessment Report of the Intergovernmental Panel on Climate Change*. Cambridge University Press, Cambridge
- IPCC (2021) *Climate change 2021: the physical science basis. Contribution of Working Group I to the Sixth Assessment Report of the Intergovernmental Panel on Climate Change*. Cambridge University Press, Cambridge
- Iturbide M, Fernández J, Gutiérrez JM et al (2021) Repository supporting the implementation of FAIR principles in the IPCC-WG1 Atlas. Zenodo. <https://doi.org/10.5281/zenodo.3691645>

- Ivory SJ, McGlue MM, Spera S et al (2019) Vegetation, rainfall, and pulsing hydrology in the Pantanal, the world's largest tropical wetland. *Environ Res Lett.* <https://doi.org/10.1088/1748-9326/ab4ffe>
- de Jesus EM, da Rocha RP, Crespo NM et al (2021) Future climate trends of subtropical cyclones in the South Atlantic basin in an ensemble of global and regional projections. *Clim Dyn.* <https://doi.org/10.1007/s00382-021-05958-8>
- Langerwisch F, Rost S, Gerten D et al (2013) Potential effects of climate change on inundation patterns in the Amazon Basin. *Hydrol Syst Sci* 17:2247–2262. <https://doi.org/10.5194/hess-17-2247-2013>
- Langerwisch F, Walz A, Rammig A et al (2016) Deforestation in Amazonia impacts riverine carbon dynamics. *Earth Syst Dyn* 7:953–968. <https://doi.org/10.5194/esd-7-953-2016>
- Lázaro WL, Oliveira-Júnior ES, Silva CJ et al (2020) Climate change reflected in one of the largest wetlands in the world: an overview of the Northern Pantanal water regime. *Acta Limnol Bras.* <https://doi.org/10.1590/S2179-975X7619>
- Leggett J, Pepper WJ, Swart RJ et al (1992) Emissions scenarios for the IPCC: an update. In: Houghton JT, Callander BA, Varney SK (eds) WMO/UNEP Intergovernmental Panel on Climate Change 1992—the supplementary report to the IPCC scientific assessment, pp 75–95
- Li C, Zwiers F, Zhang X et al (2021) Changes in annual extremes of daily temperature and precipitation in CMIP6 models. *J Clim* 34:3441–3460. <https://doi.org/10.1175/JCLI-D-19-1013.1>
- Llopart M, Coppola E, Giorgi F et al (2014) Climate change impact on precipitation for the Amazon and La Plata basins. *Clim Change* 125:111–125. <https://doi.org/10.1007/s10584-014-1140-1>
- Llopart M, Reboita M, Coppola et al (2018) Land use change over the Amazon forest and its impact on the local climate. *Water.* <https://doi.org/10.3390/w10020149>
- López-Franca N, Zaninelli P, Carril A et al (2016) Changes in temperature extremes for 21st century scenarios over South America derived from a multi-model ensemble of regional climate models. *Clim Res* 68:151–167. <https://doi.org/10.3354/cr01393>
- Magalhães AR (2016) Life and drought in Brazil. In: De Nys E, Engle NL, Magalhães AR (eds) *Drought in Brazil—proactive management and policy.* CRC Press, Boca Raton, pp 1–18. <https://doi.org/10.1201/9781315367415>
- Manabe S, Bryan K (1969) Climate calculations with a combined ocean-atmosphere model. *J Atmos Sci* 26:786–789. [https://doi.org/10.1175/1520-0469\(1969\)026%3c0786:CCWACO%3e2.0.CO;2](https://doi.org/10.1175/1520-0469(1969)026%3c0786:CCWACO%3e2.0.CO;2)
- Marengo JA, Torres RR, Alves LM (2017) Drought in Northeast Brazil—past, present, and future. *Theor Appl Climatol* 129:1189–1200. <https://doi.org/10.1007/s00704-016-1840-8>
- Marengo JA, Alves LM, Soares WR et al (2013) Two contrasting severe seasonal extremes in tropical South America in 2012: flood in Amazonia and drought in Northeast Brazil. *J Clim* 26:9137–9154. <https://doi.org/10.1175/JCLI-D-12-00642.1>
- Marengo JA, Souza CM, Thonicke K et al (2018) Changes in climate and land use over the Amazon region: current and future variability and trends. *Front Earth Sci.* <https://doi.org/10.3389/feart.2018.00228>
- Marengo JA, Cunha APMA, Nobre CA et al (2020) Assessing drought in the drylands of northeast Brazil under regional warming exceeding 4 °C. *Nat Hazards* 103:2589–2611. <https://doi.org/10.1007/s11069-020-04097-3>
- Marengo JA, Camarinha PI, Alves LM et al (2021a) Extreme rainfall and hydro-geo-meteorological disaster risk in 1.5, 2.0, and 4.0°C global warming scenarios: an analysis for Brazil. *Front Clim.* <https://doi.org/10.3389/fclim.2021.610433>
- Marengo JA, Cunha AP, Cuartas LA et al (2021b) Extreme drought in the Brazilian Pantanal in 2019–2020: characterization, causes, and impacts. *Front Water.* <https://doi.org/10.3389/frwa.2021.639204>
- Marengo JA, Galdos MV, Challinor A et al (2021c) Drought in Northeast Brazil: a review of agricultural and policy adaptation options for food security. *Clim Resilience Sustain.* <https://doi.org/10.1002/cli2.17>

- Marrafon VH, Reboita MS, da Rocha RP et al (2022) Classificação dos tipos de ciclones sobre o Oceano Atlântico Sul em projeções com o RegCM4 E MCGs. *Rev Bras Climatol.* <https://doi.org/10.55761/abclima.v30i18.14603>
- McKee TB, Doesken NJ, Kleist J (1993) The relationship of drought frequency and duration to time scales. In: Proceedings of the 8th conference on applied climatology, Anaheim, CA, 17–22 Jan 1993
- McPhaden MJ, Santoso A, Cai W (2020) Introduction to El Niño Southern oscillation in a changing climate. In: McPhaden MJ, Santoso A, Cai (eds) *El Niño southern oscillation in a changing climate*. Wiley, New York, pp 3–20
- Nakicenovic N, Alcamo J, Davis G et al (2000) Special report on emissions scenarios: a special report of Working Group III of the Intergovernmental Panel on Climate Change. Cambridge University Press, Cambridge
- Naumann G, Podesta G, Marengo J et al (2021) The 2019–2021 extreme drought episode in La Plata Basin. European Union, Luxembourg. <https://doi.org/10.2760/773>
- Nobre CA, Sampaio G, Borma LS et al (2016) Land-use and climate change risks in the Amazon and the need of a novel sustainable development paradigm. *PNAS* 113:10759–10768. <https://doi.org/10.1073/pnas.1605516113>
- Paca VHM, Espinoza-Dávalos GE, Moreira DM et al (2020) Variability of trends in precipitation across the Amazon River basin determined from the CHIRPS precipitation product and from station records. *Water.* <https://doi.org/10.3390/w12051244>
- Pfahl S, O’Gorman PA, Fischer EM (2017) Understanding the regional pattern of projected future changes in extreme precipitation. *Nat Clim Change* 7:423–427. <https://doi.org/10.1038/nclimate3287>
- Pinho PF, Marengo JA, Smith MS (2015) Complex socio-ecological dynamics driven by extreme events in the Amazon. *Reg Environ Change* 15:643–655. <https://doi.org/10.1007/s10113-014-0659-z>
- Pivello VR, Vieira I, Christianini AV et al (2021) Understanding Brazil’s catastrophic fires: causes, consequences and policy needed to prevent future tragedies. *Perspect Ecol Conserv* 19:233–255. <https://doi.org/10.1016/j.pecon.2021.06.005>
- Reboita MS, da Rocha RP, Dias CG et al (2014) Climate projections for South America: RegCM3 driven by HadCM3 and ECHAM5. *Adv Meteorol.* <https://doi.org/10.1155/2014/376738>
- Reboita MS, Ambrizzi T, Silva BA et al (2019) The South Atlantic subtropical anticyclone: present and future climate. *Front Earth Sci.* <https://doi.org/10.3389/feart.2019.00008>
- Reboita MS, Ambrizzi T, Crespo NM et al (2021a) Impacts of teleconnection patterns on South America climate. *Ann N Y Acad Sci* 1504:116–153. <https://doi.org/10.1111/nyas.14592>
- Reboita MS, Crespo NM, Dutra LMM et al (2021b) Iba: the first pure tropical cyclogenesis over the Western South Atlantic Ocean. *J Geophys Res: Atmos.* <https://doi.org/10.1029/2020JD033431>
- Reboita MS, Crespo NM, Torres JA et al (2021c) Future changes in winter explosive cyclones over the Southern Hemisphere domains from the CORDEX-CORE ensemble. *Clim Dyn* 57:3303–3322. <https://doi.org/10.1007/s00382-021-05867-w>
- Reboita MS, Kuki CAC, Marrafon VH et al (2021d) South America climate change revealed through climate indices projected by GCMs and Eta-RCM ensembles. *Clim Dyn.* <https://doi.org/10.1007/s00382-021-05867-w>
- Reboita MS, Reale M, da Rocha RP et al (2021e) Future changes in the wintertime cyclonic activity over the CORDEX-CORE southern hemisphere domains in a multi-model approach. *Clim Dyn* 57:1533–1549. <https://doi.org/10.1007/s00382-020-05317-z>
- Reichstein M, Bahn M, Ciais P et al (2013) Climate extremes and the carbon cycle. *Nature* 500:287–295. <https://doi.org/10.1038/nature12350>
- Schöngart J, Junk WJ (2020) Clima e hidrologia nas várzeas da Amazônia Central. In: Junk WJ, Piedade MTF, Wittmann F et al (eds) *Várzeas Amazônicas Desafios para um Manejo Sustentável*, pp 44–65
- Science Panel for the Amazon 2021. Executive Summary of the Amazon Assessment Report 202. United Nations Sustainable Development Solutions Network, New York, USA

- Seneviratne SI, Zhang X, Adnan A et al (2021) Weather and climate extreme events in a changing climate. In: Masson-Delmotte BZ, Zhai VP, Pirani A (eds) *Climate change 2021: the physical science basis. Contribution of Working Group I to the Sixth Assessment Report of the Intergovernmental Panel on Climate Change*. Cambridge University Press. <https://www.ipcc.ch/report/sixth-assessment-report-working-group-i/>. Accessed 14 Dec 2022
- Shepherd TG (2014) Atmospheric circulation as a source of uncertainty in climate change projections. *Nat Geosci* 7:703–708. <https://doi.org/10.1038/ngeo2253>
- Shukla PR, Skea J, Calvo Buendia E et al (2019) *Climate change and land: an IPCC special report on climate change, desertification, land degradation, sustainable land management, food security, and greenhouse gas fluxes in terrestrial ecosystems*. <https://www.ipcc.ch/srccl/>. Accessed 14 Dec 2022
- Sun Q, Zwiers F, Zhang X et al (2020) A comparison of intra-annual and long-term trend scaling of extreme precipitation with temperature in a large-ensemble regional climate simulation. *J Clim* 33:9233–9245. <https://doi.org/10.1175/JCLI-D-19-0920.1>
- Teichmann C, Jacob D, Remedio AR et al (2021) Assessing mean climate change signals in the global CORDEX-CORE ensemble. *Clim Dyn* 57:1269–1292. <https://doi.org/10.1007/s00382-020-05494-x>
- Teodoro TA, Reboita MS, Llopart M et al (2021) Climate change impacts on the South American Monsoon System and its surface-atmosphere processes through RegCM4 CORDEX-CORE projections. *Earth Syst Environ* 5:825–847. <https://doi.org/10.1007/s41748-021-00265-y>
- Trenberth KE (2020) ENSO in the global climate system. In: McPhaden MJ, Santoso A, Cai (eds) *El Niño southern oscillation in a changing climate*. Wiley, New York, pp 21–37
- Trenberth KE, Fasullo JT, Shepherd TG (2015) Attribution of climate extreme events. *Nat Clim Change* 5:725–730. <https://doi.org/10.1038/nclimate2657>
- Trenberth KE, Branstator GW, Karoly D et al (1998) Progress during TOGA in understanding and modeling global teleconnections associated with tropical sea surface temperatures. *J Geophys Res—Oceans* 103:14291–14324. <https://doi.org/10.1029/97JC01444>
- Vendruscolo J, Perez Marin AM, Santos Felix E et al (2021) Monitoring desertification in semiarid Brazil: using the Desertification Degree Index (DDI). *Land Degrad Dev* 32:684–698. <https://doi.org/10.1002/ldr.3740>
- Van Vuuren DP, Stehfest E, Den Elzen MGJ, et al (2011) RCP2.6: Exploring the possibility to keep global mean temperature change below 2°C. *Clim Change*. <https://doi.org/10.1007/s10584-011-0152-3>
- Vieira RMSP, Sestini MF, Tomasella J et al (2020) Characterizing spatio-temporal patterns of social vulnerability to droughts, degradation and desertification in the Brazilian northeast. *Environ Sustain Indic*. <https://doi.org/10.1016/j.indic.2019.100016>
- Wang C, Deser C, Yu JY et al (2017) El Niño and Southern Oscillation (ENSO): a review. In: Glynn PW, Manzello DP, Enochs IC (eds) *Coral reefs of the eastern tropical Pacific*. Springer, Amsterdam, pp 85–106
- Wang XY, Li X, Zhu J et al (2018) The strengthening of Amazonian precipitation during the wet season driven by tropical sea surface temperature forcing. *Environ Res Lett* 13:94015. <https://doi.org/10.1088/1748-9326/aadbb9>
- Zhang W, Jiang F, Stuecker MF et al (2021) Spurious North Tropical Atlantic precursors to El Niño. *Nat Commun*. <https://doi.org/10.1038/s41467-021-23411-6>